Inhibiting and reversing amyloid-beta peptide (1-40) fibril formation with gramicidin S and engineered analogues

Luo, J.H.; Otero, J.M.; Yu, C.H.; Warmlander, S.K.T.S.; Graslund, A.; Overhand, M.; Abrahams, J.P.

CHEMISTRY
A EUROPEAN JOURNAL

ChemPubSoc
Europe

DOI: 10.1002/chem.201301535

Inhibiting and Reversing Amyloid-β Peptide (1–40) Fibril Formation with Gramicidin S and Engineered Analogues

Jinghui Luo,[a] José M. Otero,*[a, b] Chien-Hung Yu,[a] Sebastian K. T. S. Wärmländer,[c] Astrid Gräslund,[c] Mark Overhand,[a] and Jan Pieter Abrahams*[a]

Abstract: In Alzheimer's disease, amyloid-β (Aβ) peptides aggregate into extracellular fibrillar deposits. Although these deposits may not be the prime cause of the neurodegeneration that characterizes this disease, inhibition or dissolution of amyloid fibril formation by Aβ peptides is likely to affect its development. ThT fluorescence measurements and AFM images showed that the natural antibiotic gramicidin S significantly inhibited Aβ amyloid formation in vitro and could dissolve amyloids that had formed in the absence of the antibiotic. In silico docking suggested that gramicidin S, a cyclic decapeptide that adopts a β-sheet conformation, binds to the Aβ peptide hairpin-stacked fibril through β-sheet interactions. This may explain why gramicidin S reduces fibril formation. Analogues of gramicidin S were also tested. An analogue with a potency that was four-times higher than that of the natural product was identified.

Keywords: Alzheimer's disease · amyloid-beta peptides · antibiotics · fibrillization · structure–activity relationships

Introduction

Protein amyloid fibrils are found to be closely associated with several neurodegenerative pathologies, such as Alzheimer's,[1] Huntington's,[2] and Parkinson's[3] diseases, as well as diabetes mellitus type 2[4] and transmissible spongiform encephalopathies.[5] More than 30 proteins with quite different sequences and structures have been identified in the development of amyloidogenic processes related to neurodegenerative diseases. Main-chain hydrogen bonds through β-sheet interactions between (peptide segments of) these proteins are the main driving force in the fibril formation. The insoluble fibrillar peptides that result are deposited in the intraneuronal space, which affects neuromuscular signaling by disrupting factors controlling synaptic dopamine homeostasis.[6,7] Several approaches have been identified to prevent the formation of amyloid fibrils.[8,9] One of these approaches uses the fibril-forming segment peptide from the self protein as an inhibitor.[10–13] Furthermore, non-natural peptides have been designed as macrocyclic β-sheet mimics to disrupt the fibril formation.[14–21] Recently, a series of macrocyclic β-sheet peptides were synthesized and modified to prove their ability to inhibit the aggregation of a tau-protein-derived peptide,[14] and a series of cyclic non-natural amino acid inhibitors were designed against amyloid fibril formation based on the structure of the amyloid "zipper" model.[15,16] In addition, aromatic compounds such as dopamine, Congo red, and curcumin can be used to inhibit the protein aggregation.[22] Crystal structures of aromatic compounds and hexapeptide "zipper" complexes indicate inhibition of amyloid fibril formation through interference with the hydrophobic β-sheets of the aggregates.[23]

The fibrillization of amyloid-β (Aβ) peptide is recognized as an important step in the course of Alzheimer's disease.[24] A part of the 3D structure of the Aβ(1–42) fibril has been solved by solid-state NMR spectroscopy.[25] Residues 1–17 are disordered and do not appear in the 3D model. Residues 18–42 form a hairpin-like structure with a β1-strand (18–26)–turn–β2-strand (31–42) motif (Figure 1a). At least two molecules are required to obtain a protofilament structure through the parallel packing of the β-strands. The Aβ(18–42) peptide contains 20 apolar amino acids (5 Val, 5 Gly, 3 Ala, 3 Ile, 2 Phe, 1 Leu, and 1 Met) and five polar amino acids (Glu, Asp, Ser, Asn, and Lys). Intermolecular side-chain contacts involved in the protofilament generation are formed between residues from the β1-strand of one molecule and residues from the β2-strand of the adjacent molecule. In addition, N–H→O=C intermolecular hydrogen bonds from parallel β-sheets are formed between equivalent

[a] J. Luo, Dr. J. M. Otero, Dr. C.-H. Yu, Prof. M. Overhand, Prof. J. P. Abrahams
Leiden Institute of Chemistry, Leiden University
Einsteinweg 55, 2333 CC, Leiden (The Netherlands)
E-mail: jose.otero@usc.es
abrahams@chem.leidenuniv.nl

[b] Dr. J. M. Otero
Departamento de Bioquímica y Biología Molecular
Facultad de Farmacia y Centro Singular de Investigación en Química Biológica y Materiales Moleculares (CIQUS)
Campus Vida, Universidad de Santiago de Compostela
15782 Santiago de Compostela (Spain)

[c] Dr. S. K. T. S. Wärmländer, Prof. A. Gräslund
Department of Biochemistry and Biophysics
The Arrhenius Laboratories for Natural Sciences
Stockholm University, 10691 Stockholm (Sweden)

Supporting information for this article is available on the WWW under http://dx.doi.org/10.1002/chem.201301535.

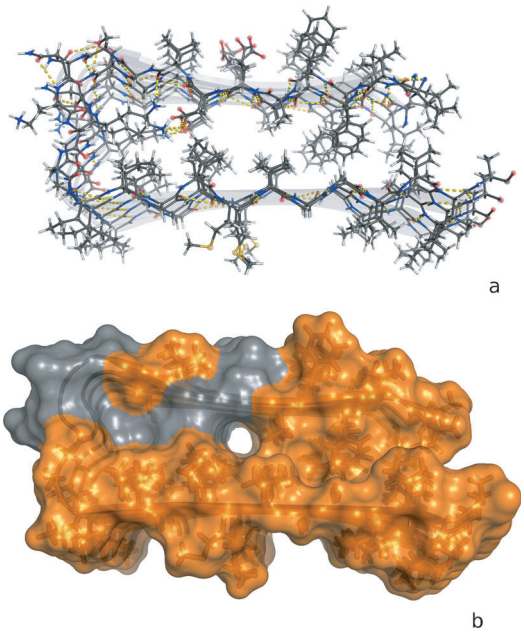

Figure 1. The 3D structure of the Aβ(17–42) fibril with a β-hairpin-like motif and intermolecular β-sheet interactions. a) Yellow dotted lines are hydrogen bonds among five repeated hairpin-like structures. b) Orange and gray cartoon represents the hydrophobic and hydrophilic surfaces, respectively. All figures were made with the PyMOL software (PDB ID: 2BEG).

β-strands in the protofilament structure (Figure 1). An intermolecular salt bridge is formed between Asp23 and Lys28 from adjacent molecules. The charged residues (Glu22, Asp23, and Lys28) are in the corner of the hairpin-like structure, with the rest of the structure having hydrophobic side chains. A channel is located in the middle of the hairpin-like structure between the hydrophobic and hydrophilic surfaces (Figure 1b).

The formation of Aβ fibrils and other β-sheet-rich derivative macrostructures can be inhibited by macrocyclic peptides designed to adopt adequate β-sheet structures for binding to incipient protofilament structures.[20] So far, only the inhibition of fibril formation by cyclic peptides has been described, but the dissolution of preformed amyloid cyclic peptides has not yet been demonstrated. Unfortunately, the great variation in the amino acid sequences of the peptides associated with neurodegenerative diseases impedes the design of wide-ranging drugs that interfere with neurotoxic amyloid formation. Compounds that are able to interfere with Aβ peptide aggregation without the need to recognize specific amino acid sequences would pave a promising way for generating drugs against a broad range of neurodegenerative diseases.

Gramicidin S (GS, **1**) is an antibacterial derivative that is active against a broad range of Gram-positive bacteria, certain Gram-negative bacteria, and some fungi.[26,27] However, its clinical applications are limited to topical uses like ear infections,[28] because GS is toxic for human red blood cells by causing hemolysis. Recent studies have shown that the hemolytic activity of GS-based compounds can be tuned through modifications in the amino acid sequence; this has given rise to GS derivatives with decreased hemolytic properties, which retain antibacterial activity and the clinical applications of which as antibiotics are currently under investigation.[29,30]

The natural product GS (cyclo-(Val-Orn-Leu-D-Phe-Pro)$_2$) is a symmetrical macrocyclic decapeptide that was isolated for the first time from the bacterium *Aneurinibacillus migulanus* (*Bacillus brevis*).[31,32] Its secondary structure has an extended β-sheet conformation formed by two antiparallel β-strands (Val-Orn-Leu) interconnected by two type II′ β-turns (D-Phe-Pro). Four interstrand hydrogen bonds stabilize a special arrangement of the amino acids, with the hydrophobic amino acids side chains (Leu and Val) oriented to one side of the β-sheet and the polar side chains (Orn) on the opposite side, which makes GS an amphiphilic molecule (Figure 2).[33,34] Structural studies of native GS (**1**) and the analogues **4**–**8** (see Figures 5 and 9) with ^{1}H and ^{13}C NMR spectroscopy were described in recent papers.[29,34–36] The dispersion of the amide proton signals in the ^{1}H NMR spectrum indicated that there are no multiple conformations in solution, and the observed chemical shifts, coupling constants, and nuclear Overhauser effects demon-

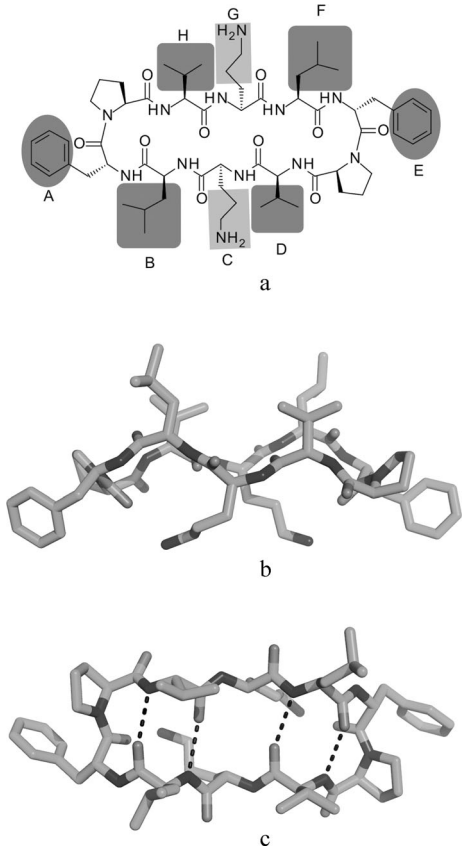

Figure 2. The chemical structure of gramicidin S (**1**). a) It consists of two identical, cyclically linked pentapeptides, namely, cyclo-(Val-Orn-Leu-D-Phe-Pro)$_2$. b) Crystallographic amphiphilic structure with a hydrophobic face (top) and a hydrophilic face (bottom). c) Detail of the four interstrand hydrogen bonds (dotted lines) involved in the β-sheet stabilization.

strated that this conformation corresponds to a stable cyclic β-hairpin configuration. The ^{1}H and ^{13}C NMR spectra for analogues **2** and **3** (see Figure 7) showed multiple signals per nucleus, which indicates that they exist in solution as multiple interchanging conformations, and although they have similar structures to gramicidin S, we cannot be certain that they adopt β-hairpin conformations.

Herein, we show by thioflavin T (ThT) fluorescence assays and scanning probe microscopy that the natural antibiotic GS effectively inhibits the formation of Aβ peptide fibrils. From in silico docking studies, we infer the binding site of GS in the Aβ fibril to be located in the channel between the hydrophobic and hydrophilic interfaces. These findings prompted us to investigate and further characterize the interaction between GS analogues and the Aβ peptide.

Experimental Section

Synthesis of gramicidin S and analogues: The synthesis, characterization, and crystallographic structural studies of gramicidin S (**1**) and GS analogues **4**–**8** were previously reported in the literature.[34–36] GS analogues **2** and **3** were synthesized with an adaptation of a previously reported method.[30] All peptides were synthesized by using a standard 9-fluorenylmethoxycarbonyl (Fmoc) protection peptide synthesis protocol, involving the assembly of the protected linear decapeptides on a solid support, mild acidic cleavage, and macrocyclization in solution by using PyBOP/HOBt/DiPEA in DMF at high dilution. Complete deprotection of the cyclopeptides followed by preparative reversed-phase HPLC purification allowed 20–40% overall yields of compounds **1**–**8** as fluffy white solids after lyophilization. (For details, see the Supporting Information).

Aβ peptides preparation: The 40 and 42 amino acid amyloid-β peptides (Aβ(1–40) and Aβ(1–42), respectively) were bought from AlexoTech AB (Umeå, Sweden) and prepared according to previously described protocols.[37] The peptides were dissolved in 10 mM NaOH to a peptide concentration of 2 mg mL^{-1} and then sonicated for 1 min in an ice bath before dilution in the appropriate buffer. The preparations were kept over ice.

ThT assay: *Inhibition assay*: A 10 mM ThT stock solution was prepared in 50 mM tris(hydroxymethyl)aminomethane (Tris) buffer (pH 7.4) and filtered to remove ThT particles. GS (**1**) or one of the GS analogues (**2**–**8**) was added to aliquots of this solution and then freshly prepared Aβ peptide was added, to yield final samples containing 5 μM ThT, 10 μM Aβ(1–40), 50 mM Tris buffer, and 20, 50, or 100 μM GS or GS analogue. All buffers and samples were prepared over ice. The samples were pipetted into a plate with 384 wells, with each well holding 45 μL. Fluorescence measurements were recorded with an Infinite M1000 PRO microplate reader every 15 min for 17 h, by using excitation and emission wavelengths of 446 and 490 nm, respectively. The plate was held at 37 °C, and the wells were automatically shaken 30 s before each measurement. Each sample was prepared in duplicate, and the average fluorescence signals were calculated. (For details, see the Supporting Information).

Dissolution assay: Stock fibrils of the Aβ(1–40) peptide were produced by incubating 50 μM Aβ(1–40) peptide in 50 mM Tris (pH 7.4) at 37 °C with shaking at 220 rpm for 24 h. (This was the same procedure as that used for AFM sample preparation.) The aggregates were diluted to 10 μM and mixed with ThT and 10, 30, 60, or 100 μM GS (**1**) or GS analogues (**2**–**8**) for the dissolution assay. The protocol and buffer conditions were the same as those for the inhibition assay. The fluorescence was measured after the incubation at 37 °C for 17 h.

Atomic force microscopy: Samples of 50 μM Aβ(1–40) peptide in the same buffer (50 mM Tris, pH 7.4) as that used for the ThT assay were incubated at 37 °C with and without GS (**1**, 10.0 equiv) in a shaker operating at 220 rpm for 24 h. The incubated samples were then deposited on freshly cleaved mica. After 5 min, the excess liquid was shaken off, and the mica plates with deposited sample were rinsed once with 50 mM Tris buffer (pH 7.4) and dried in a stream of dry nitrogen at room temperature. The specimens were then mounted on a multimode atomic force microscope (The Digital Instruments Nanoscope III), and images were collected in tapping mode at frequencies of around 70 kHz. The imaging was carried out in air, by using silicon cantilevers with an asymmetric tip and a force constant of 3 N m^{-1}.

NMR spectroscopy: A Bruker Avance 500 MHz spectrometer was used to record the ^{1}H–^{15}N HSQC spectra of 100 μM ^{15}N-labeled Aβ(1–40) peptide in 20 mM sodium phosphate buffer at pH 7.3 (H_2O/D_2O, 90:10), both in the absence and presence of 300 μM GS (**1**). The spectrometer was equipped with a triple-resonance cryogenically cooled probe head, and the spectra were referenced to the water signal. All NMR measurements were done at 5 °C to slow down the aggregation process. The assignment of the amide cross-peaks for the Aβ(1–40) peptide is known from previous work.[37]

Dynamic light scattering (DLS): DLS experiments were performed on a Malvern instrument (Zetasizer). At least 20 measurements, each of 10 s duration were executed for each sample. Samples were incubated for 4 h at 37 °C before being transferred to ZEN0040 disposable microcuvettes (40 μL) for DLS measurements. The measurements were performed at 37 °C after 120 s of equilibrium time. The distribution of the hydrodynamic radii of particles in the solution was analyzed with the software provided by the manufacturer.

Molecular docking: The Autodock 4.2 software was used to dock GS (**1**) and GS analogues **4** and **5** to a model system of Aβ hairpin-stacked fibrils. The structure of the Aβ hairpin-stacked fibrils was downloaded from the Protein Data Bank (file: 2BEG), and the structures of GS (**1**)[34] and the GS analogues **4**[35] and **5**[36] were downloaded from the Cambridge Crystallographic Data Centre (IDs: gramsn4n, CCDC 805623, and CCDC 910309, respectively). The Lamarckian Genetic Algorithm was used to search for energetically supported binding modes. The run number was 100, and 250000 energy evaluations were applied for each run. The AutoDockTools 1.5.4 software was used to build an Autogrid box between the protein and ligands. The grid center was chosen in the center of the hairpin-like structure, and the dimensions of the grid were 90×90×90 autogrid points (*x*, *y*, and *z* directions) with 0.375 Å spacing. Only the atoms of the side chains of the ligands were set as active torsions during docking.[38,39]

Results and Discussion

Inhibition of amyloid fibril formation and disaggregation of amyloid fibrils by gramicidin S (1): Thioflavin T (ThT) binds to peptide amyloid aggregates, which results in an increase of ThT fluorescence. Figure 3a shows that the Aβ(1–40) peptide aggregated within 10–17 h without GS (black line). By contrast, the incubation of GS (**1**) alone with ThT led to no increase in fluorescence (red line). In the presence of different concentrations of GS, the amyloid aggregation of the 10 μM Aβ peptide was inhibited. The maximum fluorescence increase of the aggregates was reduced significantly in presence of 20 μM GS (green line). In the presence of 50 μM and 100 μM GS (dark blue and cyan lines, respectively), the fluorescence signal was reduced even more, which suggests significant inhibition of peptide amyloid aggregation. The absolute values of the fluorescence plateaus were not precisely reproducible in all cases (see the Supporting Information), but the trends were very clear. This variability must be inherent to the characterization of aggregation.[14,15] We verified that the absorbance of GS and its analogues did not interfere with the excitation and emission wavelengths used

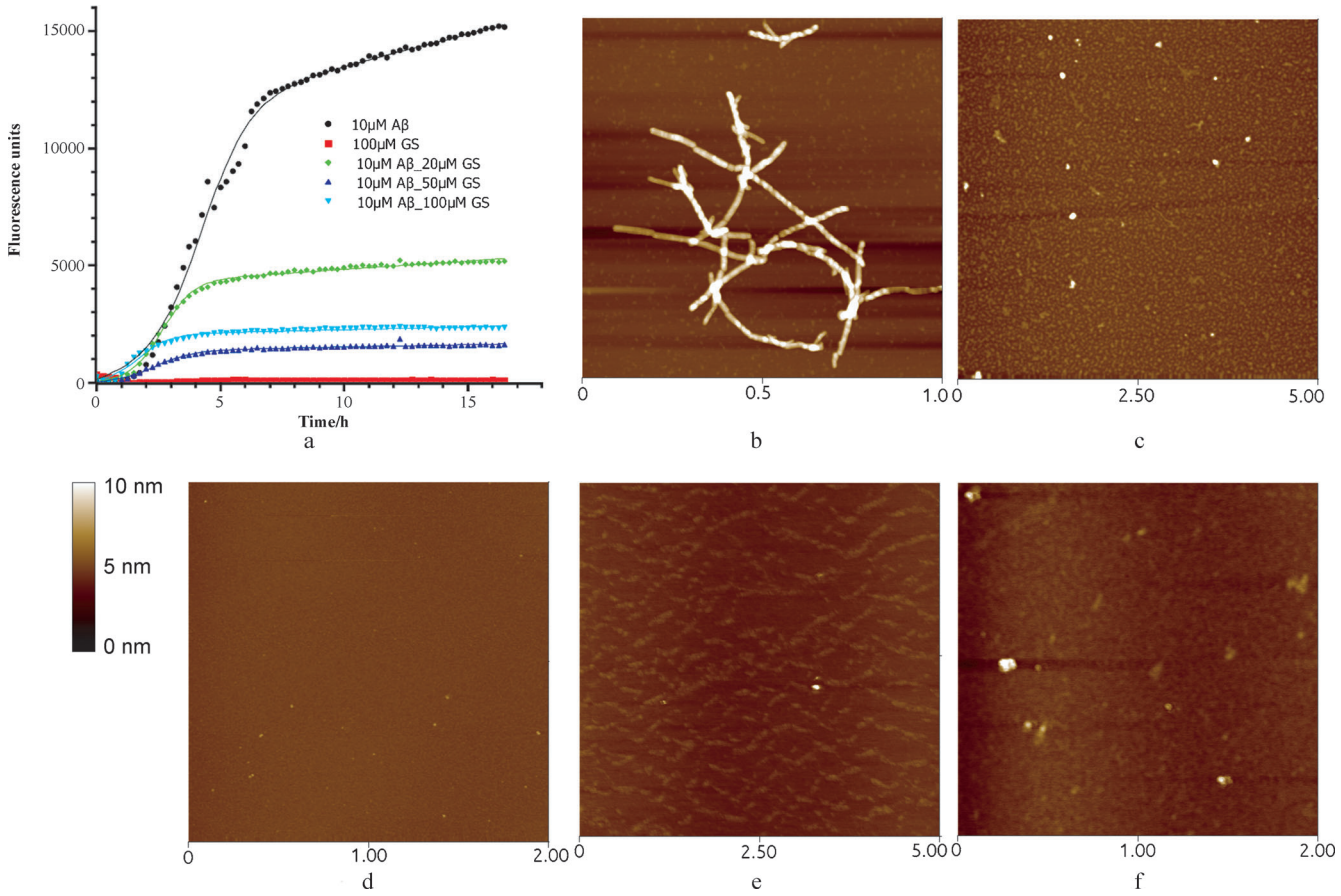

Figure 3. a) Aβ(1–40) aggregation and inhibition measured by a ThT fluorescence assay in the absence and presence of GS (**1**) at concentrations of 20, 50, and 100 μM. Atomic force microscopy images of: b) 50 μM Aβ(1–40) aggregated peptide, c) 100 μM **1**, d) a mixture of 50 μM Aβ(1–40) peptide and 100 μM **1**, e) 500 μM **1**, and f) a mixture of 50 μM Aβ(1–40) peptide and 500 μM **1**. All samples were incubated at 37 °C for 24 h.

for the ThT assay (see Figure 3 in the Supporting Information). The ThT assays were confirmed by AFM, which is a common tool for characterizing peptide fibrils and their morphologies.[40,41] AFM images obtained with samples of Aβ(1–40) peptide in the absence of GS (Figure 3b) showed the formation of large amorphous aggregates, which confirmed the fibrillization of the peptide under the assay conditions. AFM images developed with samples of Aβ(1–40) peptide in the presence of GS (**1**; Figure 3d and f) showed no formation of amyloid fibrils, which confirmed the anti-aggregating activity of GS in these assays. As controls, samples of GS at the same concentrations as those used for the inhibition assays were analyzed by AFM (Figure 3c and e). These images showed the formation of some small aggregates, which indicated the formation of macromolecular GS associations that are probably the same as or similar to those previously described in the literature.[42]

The proposed interactions between gramicidin S (1) and Aβ fibrils: The details of the interactions between Aβ peptide fibrils and small molecules are unknown because there is no high-resolution structure of fibrils, although a hollow-core structure of the Aβ(1–42) peptide was observed by cryoelectron microscopy.[43] The potential interaction between the monomer Aβ(1–40) peptide and GS was studied here by NMR spectroscopy. The results suggest that there is no effect of GS on the conformation of the monomer Aβ(1–40) peptide (Figure 4a). All of the HSQC cross-peaks from the monomeric Aβ(1–40) peptide kept the same pattern before and after addition of GS, which suggests that the interaction with the amyloid fibril structures by GS might contribute to the inhibition of amyloid formation. In order to propose a possible binding site of GS (**1**) on the Aβ peptide fibril, molecular docking studies were performed. We used the Aβ-(18–42) hairpin-stacked structure, which was solved by solid-state NMR spectroscopy (Protein Data Bank file: 2BEG),[25] as the amyloid model (Figure 1). The earlier NMR data indicated the N-terminus of the Aβ(18–42) peptide to be rather flexible, and we excluded this part from our calculations. The crystallographic structure[34] of GS (Figure 2) was docked into the β-hairpin-like structure as described in the Materials and Methods section. These docking studies prompted us to propose that GS binds inside the fibrillar tube and interacts through its hydrophobic side chains (Leu and Val) with the apolar amino acids of the hydrophobic interface of the Aβ peptide (Val32 and Leu34) and through its

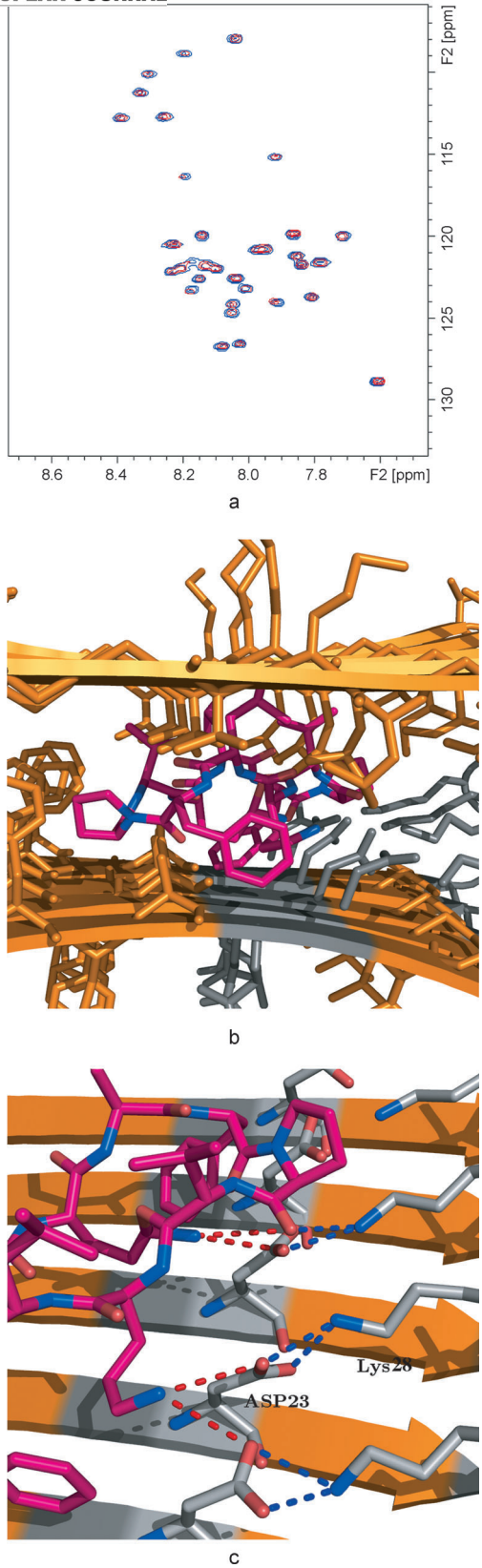

Figure 4. a) Overlaid ^{1}H–^{15}N HSQC NMR spectra of 100 μM ^{15}N-labeled Aβ(1–40) peptide in 20 mM sodium phosphate buffer, at pH 7.3 and 5 °C, before (blue) and after (red) addition of 300 μM GS (**1**). b) The interaction between GS (**1**, magenta) and the Aβ(17–42) hairpin-like structure (orange and gray) suggested by molecular docking. c) Detail of the intramolecular salt bridges between Asp23 and Lys28 of the Aβ peptide (blue dotted lines) and the intermolecular salt bridges between the Orn residue of GS (**1**) and Asp23 of the Aβ peptide (red dotted lines).

hydrophilic side chains (Orn) with the polar amino acids from the Aβ peptide hydrophilic interface (Asp23), as shown in Figure 4b and c.

We extended our docking studies to a new family of GS-based mixed $(\alpha\beta\alpha\beta\alpha)_2$ cyclopeptides that we recently developed and that form β-hairpin-like structures similar to those observed with **1** (Figure 5).[35,36] The presence of β-amino acids allows these compounds greater flexibility in the β-sheet, which implies that they can take on less rigid conformations than the original structure of GS (**1**), conformations that might fit better in the β-strand–turn–β-strand motif of the amyloid peptide. The crystallographic structures of GS analogues **4**[35] and **5**[36] (only differing in the aromatic substitution at the Phe residue in the β-turn) confirm an increased conformational repertoire for these cyclic peptides. Whereas compound **4** crystallized with a fully extended β-sheet configuration (Figure 5a–c), compound **5** adopted a folded β-sheet configuration due to a tighter intermolecular packing (Figure 5d–f). Despite the presence of β-amino acids in structures **4** and **5**, both maintained the intramolecular hydrogen-bonding pattern as observed in GS (**1**).

Docking studies with the crystallographic structures of GS analogues **4** and **5** in the Aβ(17–42) hairpin-stacked structure were performed by using the same protocol as that used for the docking of GS (**1**). The conformations of the side chains on the GS analogues were allowed to be flexible during the in silico docking. It turned out that the extended conformation of GS derivative **4** did not fit in the channel interface of the Aβ peptide (results not shown). By contrast, the bent β-sheet of GS analogue **5** found a binding site in the Aβ peptide in the channel at the interface located between the hydrophobic and hydrophilic surfaces (Figure 6a). The hydrophobic side chains from Val, Leu, and naphthylalanine of analogue **5** directly interacted with hydrophobic residues Phe19, Phe20, Ala21, Leu34, Met35, and Val36 from the Aβ(18–42) peptide. Naphthalene groups of compound **5** formed hydrophobic interactions through π-stacking with Phe19 of the hairpin-like structure (Figure 6b). The higher number of ligand–protein interactions observed in the docking of GS analogue **5** with the Aβ peptide, compared with the interactions observed with GS (**1**), indicated that this family of GS-based compounds with $(\alpha\beta\alpha\beta\alpha)_2$ amino acid sequences might fit better in the channel interface of the Aβ peptide than natural GS. We speculated that this might lead to an increased anti-aggregating activity. Additionally, these observations suggested that the aromatic group at the β-turn (positions A and E) of this family of $(\alpha\beta\alpha\beta\alpha)_2$ GS-based analogues might play an important role in the ligand–protein interaction.

Gramicidin S analogues 2 and 3: the hydrophobic and hydrophilic effects of β-strands: The hydrophobic and hydrophilic side chains of GS-based antibiotics are placed at opposite sides of the β-strand, which results in an amphiphilic character that is essential for disrupting membrane integrity.[44] The modification of the hydrophobicity or hydrophilicity of the GS side chains allowed tuning of the biological

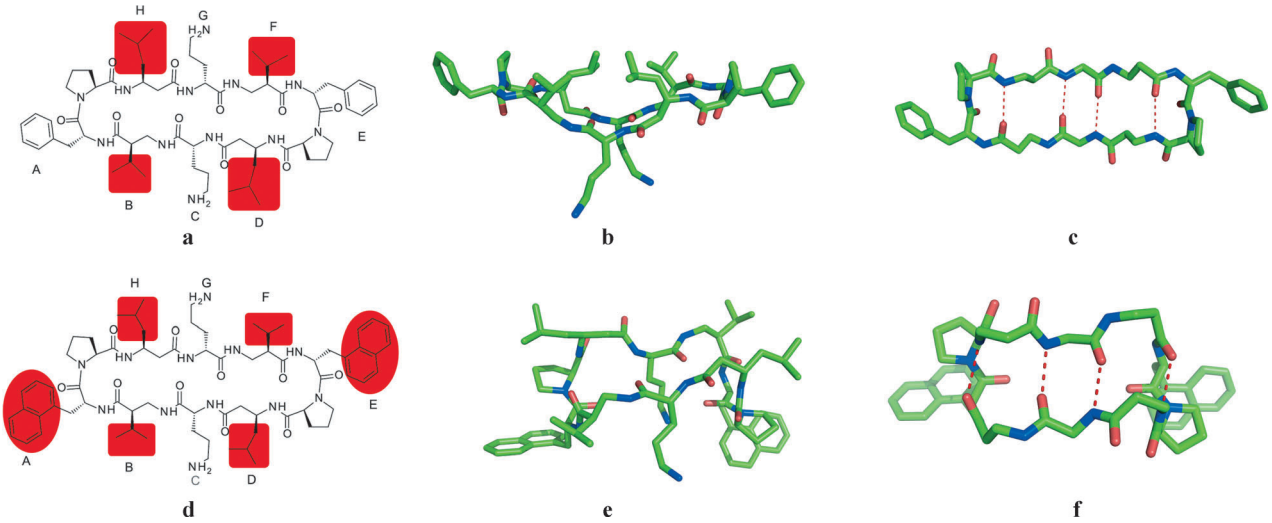

Figure 5. a), d) Chemical structures of GS analogues **4** and **5**, respectively. b), e) Side, and c), f) top views of the crystallographic structures of GS analogues **4** and **5**, respectively. Side-chains are omitted in top views for clarity; dotted lines denote hydrogen bonds.

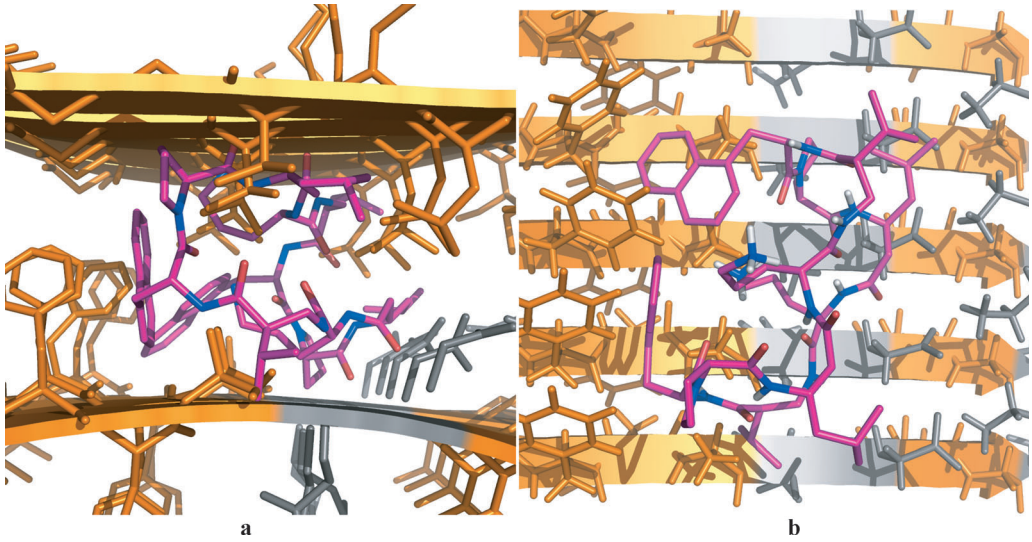

Figure 6. a) The interaction between GS analogue **5** (magenta) and the Aβ(17–42) hairpin-like structure (orange and gray) suggested by molecular docking. b) The schematic interaction between the "lower" strands of Aβ(17–42) and GS analogue **5**.

properties and allowed the preparation of molecules with a broader spectrum of antibacterial activity and reduced hemolytic activity compared to the natural compound.[29,30] Such modifications could be useful for improving the efficiency of inhibition of amyloid fibril formation, so we investigated the effect of the amphiphilic character of GS-based cyclic decapeptides on the inhibition of amyloid fibril formation. We created two new molecules with an "inverted" amphiphilic distribution, in which the hydrophobic and hydrophilic residues were exchanged (Figure 7). Hydrophilic Orn groups were used instead of hydrophobic Leu and Val groups (the B and F groups and D and H groups indicated in Figure 2, respectively), and the original Orn groups located in the center of the β-strand (the C and G groups) were replaced with hydrophobic Ala(*t*Bu) and Leu groups. In addition, one or both aromatic groups from the phenylalanines situated in the β-turns (the A and E groups) were replaced by one (compound **2**) or two (compound **3**) chains of fatty acid, respectively. This highly hydrophobic group was intended to increase the liposolubility of these GS-based derivatives, which had been heavily decreased by the inclusion of the four Orn side chains.

ThT fluorescence assays with GS-based derivatives **2** and **3** showed that, compared with the results with natural product **1**, the lag time of Aβ peptide aggregation was slightly increased in the presence of both "inverted" analogues at concentrations of 20 μM (Figure 7b and d). However, the fluorescence intensities observed in the presence of 20, 50, and 100 μM concentrations of both analogues showed that these derivatives did not completely inhibit the Aβ peptide aggre-

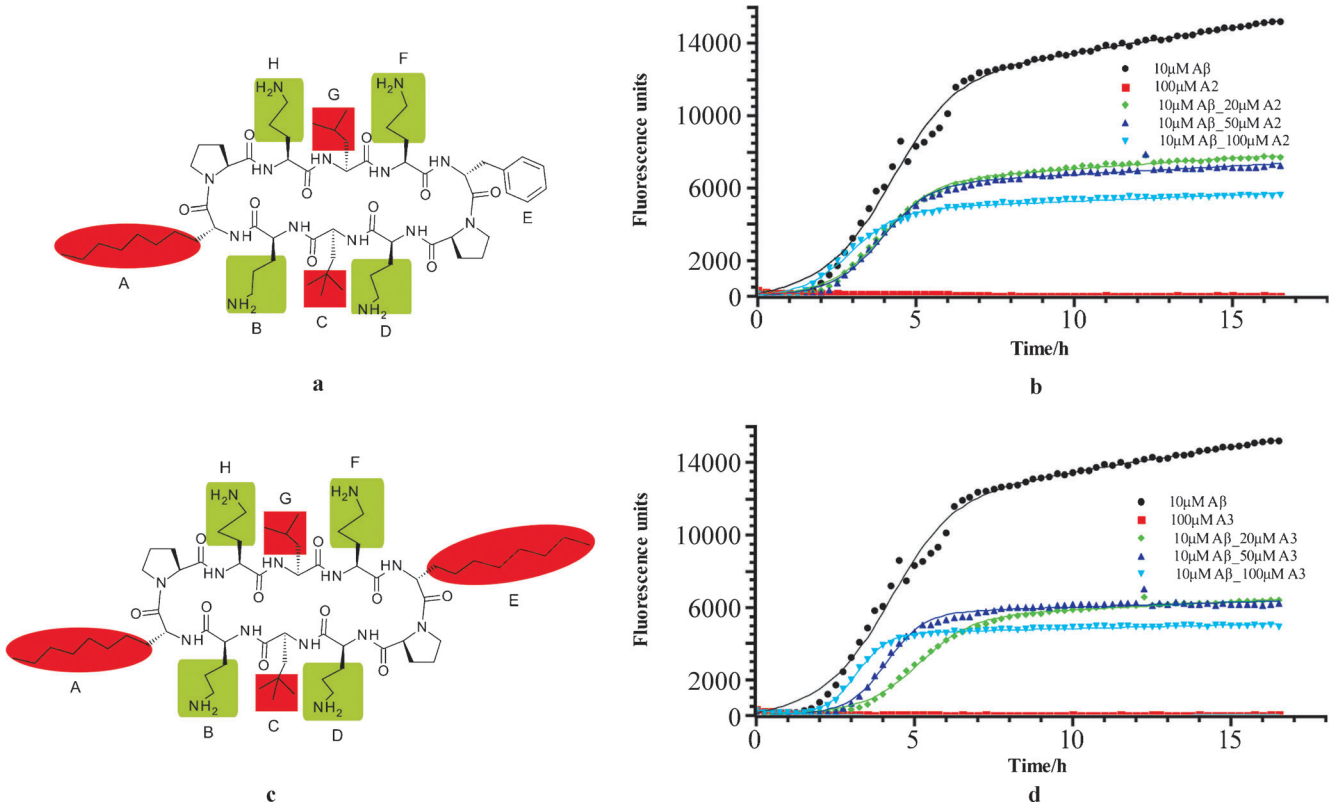

Figure 7. a), c) Structures of "inverted" GS-based analogues **2** (cyclo-(Pro-Orn-Leu-Orn-D-Phe-Pro-Orn-Ala(*t*Bu)-Orn-[(*R*)-2-Adec)]) and **3** (cyclo-(Pro-Orn-Leu-Orn-[(*R*)-2-Adec]-Pro-Orn-Ala(*t*Bu)-Orn-[(*R*)-2-Adec])), respectively. b), d) ThT fluorescence data for Aβ(1–40) aggregation and inhibition in the presence and absence of GS analogues **2** (b) and **3** (d). The concentrations of the GS analogues used in the assays were 0, 20, 50, and 100 μM, and the time scale was 17 h for each measurement.

gation, most probably due to difficulties in binding of the highly polar new surface created with the four Orn side chains to the amyloid hydrophobic structure.

Extended β-sheet gramicidin S analogues 4–8; the facial hydrophobic effects of the β-turn: Our docking studies with the $(\alpha\beta\alpha\beta\alpha)_2$ GS analogues **4** and **5** indicated that the Phe residues in the β-turns may have an important role in the binding of these molecules to the Aβ(17–42) hairpin-like structure. We therefore investigated whether the inhibition of amyloid fibrillization could be improved by replacing the Phe side chain with groups that more strongly promote π-stacking interactions. Several cyclopeptides with different aromatic functional groups attached to the β-turn were designed and synthesized, and ThT fluorescence assays were performed (Figures 8 and 9). As predicted by the docking studies, all of these compounds could completely inhibit fibril aggregation. Analogue **4**, with Phe residues in both β-turns, had a behavior similar to that of native GS (**1**; Figure 8a). In the presence of 20 μM GS analogue **4**, the lag time of aggregation (green curve) was increased relative to the results in the presence of 20 μM native GS, although the fluorescence intensity with GS analogue **4** at 50 μM (dark blue curve) is a bit higher than that observed with native GS (**1**) at the same concentration. The fibrillization disappeared at a concentration of 100 μM of compound **4** (cyan curve). When we swapped both phenyl groups of the Phe residues for 1-naphthyl groups, GS analogue **5** was obtained. In the presence of a 20 μM concentration of this compound, the kinetics of Aβ peptide amyloid aggregation changed only slightly compared to those with derivative **4** or native GS (**1**), but compound **5** is a stronger inhibitor of the Aβ(1–40) peptide aggregation at 50 μM (Figure 8b).

A stronger hydrophobic group, 9-anthracenyl, replaced the Phe side chains in derivative **6** (Figure 9a). Fibril inhibition by this derivative was less efficient than that with the naphthyl-group derivative **5**. At 20 and 50 μM, the aggregation kinetics was generally faster, and aggregates were completely suppressed only at a concentration of 100 μM (Figure 9b).

These results are consistent with our docking studies, which indicated that the two Phe groups from the GS-based derivative **4** interact with Phe groups from five different β-sheets of the Aβ peptides. The binding pocket for the GS derivatives is relatively small, and it might not be large enough for the bulky 9-anthracyl groups of compound **6**. Conversely, the smaller naphthalene group could insert more snugly into the hydrophobic pocket. This could explain why GS analogue **5** bound with higher affinity to the Aβ peptide hairpin-stacked fibrils and showed more efficient inhibition of Aβ fibril formation, as observed by ThT fluorescence, than GS analogue **6**.

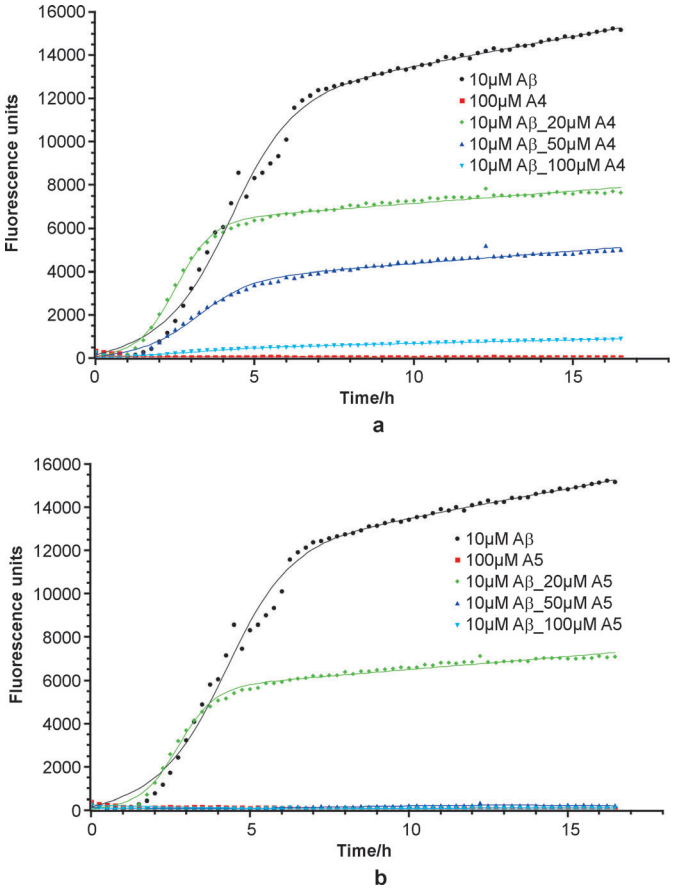

Figure 8. ThT fluorescence data for Aβ(1–40) aggregation and inhibition in presence and absence of GS analogues **4** (a) and **5** (b). The concentrations of the GS analogues were 0, 20, 50, and 100 μM, and the time scale was 17 h for each measurement.

To confirm the significance of the intermolecular π-stacking interactions between the fibrils and the GS-based derivatives' Phe groups and to consider the size of the binding pocket, we prepared two other compounds, analogues **7** and **8** (Figure 9c and e, respectively). The Phe side chains of analogue **4** (the A and E groups) were swapped with a pentafluorophenyl group and a naphthyl group, respectively, in compound **7**. The "inverted" aromatic polarity of the pentafluorophenyl group has been widely used to promote π-stacking interactions with other aromatic moieties.[45] As we expected, the ThT fluorescence due to Aβ peptide aggregation considerably decreases in the presence of a 20 μM concentration of the new GS derivative **7**, which indicated tighter binding of **7** to the Aβ(1–40) peptide. Finally, we synthesized a new GS analogue (compound **8**) with a 2-fluorenyl group instead of the naphthalene group present in derivative **7** (Figure 9e). The size of the 2-fluorenyl group is between that of the naphthyl and 9-anthracyl groups, which could optimize the anti-aggregation activity of the inhibitor. Clearly, Figure 9f illustrates a greater effect on the inhibition of the Aβ peptide aggregation in the presence of **8** than with any of the other GS-based analogues or with natural GS (**1**). These results further proved the significance of the π-stacking interactions between the aromatic groups from the β-turns in these GS-based cyclopeptides and the aromatic moieties located in the Phe clusters of the Aβ(1–40) peptide. These results also confirmed the binding mode obtained by our molecular docking simulations.

Furthermore, GS and its analogues displayed a similar inhibition of the fibrillization of the Aβ(1–42) (Figure 4a in the Supporting Information). We also performed optical density (OD) and DLS assays to compare the Aβ(1–40) peptide aggregates formed in the presence and absence of GS and its analogues (Figure 4.b and Figure 5 in the Supporting Information). We found the cluster size of the Aβ-(1–40) aggregates to be reduced and to be more monodisperse in the presence of GS or its analogues relative to the Aβ(1–40) aggregates in the absence of the compounds. The OD assays would not quantify the differences between the Aβ(1–40) aggregates in the presence and absence of GS and its analogues. DLS assays of GS and its analogues (Figure 5 in the Supporting Information) indicate the presence of aggregates of GS at the concentrations utilized. These aggregates could not be confirmed by AFM and may only represent a tiny mass fraction of the GS present (the DLS intensity scales with the cube of the particle radius). Nevertheless, the presence of aggregates may contribute to the inhibition of fibril formation, because it was reported that random aggregates of small molecules inhibited amyloid formation of the prion proteins Sup35 and recMoPrP through a process termed "colloidal inhibition".[46]

Intermolecular, parallel, and in-register β-sheets are important features of the Aβ peptide in fibril aggregation. The growth of a fibril occurs through the addition of a new peptide to the edge of its sheet, accompanied by hydrophobic interactions and the formation of hydrogen bonds at the edges of the strands.[11] Thus, inhibition of aggregation could be induced by interfering with these hydrophobic interactions and hydrogen bonds. As shown in Figure 1b, the surface of the fibril consists of a hydrophobic–hydrophilic–hydrophobic surface. Furthermore, the fibril has a channel located at the interface between the hydrophobic and hydrophilic residues, which may bind additional compounds, and our results suggest that these might include GS and its derivatives. The insertion of the GS analogues into the channel, which we propose here (on the basis of our docking studies), may distort the conformation of the fibril end sufficiently to prevent or at least hinder the addition of new peptides. GS analogue **4** could not be fitted into the channel interface as well as the other aggregates. This may explain why this analogue was less active as an inhibitor of fibrillization.

Dissolution of amyloid fibrils by gramicidin S and its analogues: We investigated whether GS and its analogues also had the potency to dissolve preformed amyloid fibrils (Figure 10). We can report that this is indeed the case. We added GS and its analogues to 10 μM samples of aggregated amyloid fibrils that had matured over a period of 24 h. In order to measure the aggregation state, we added ThT

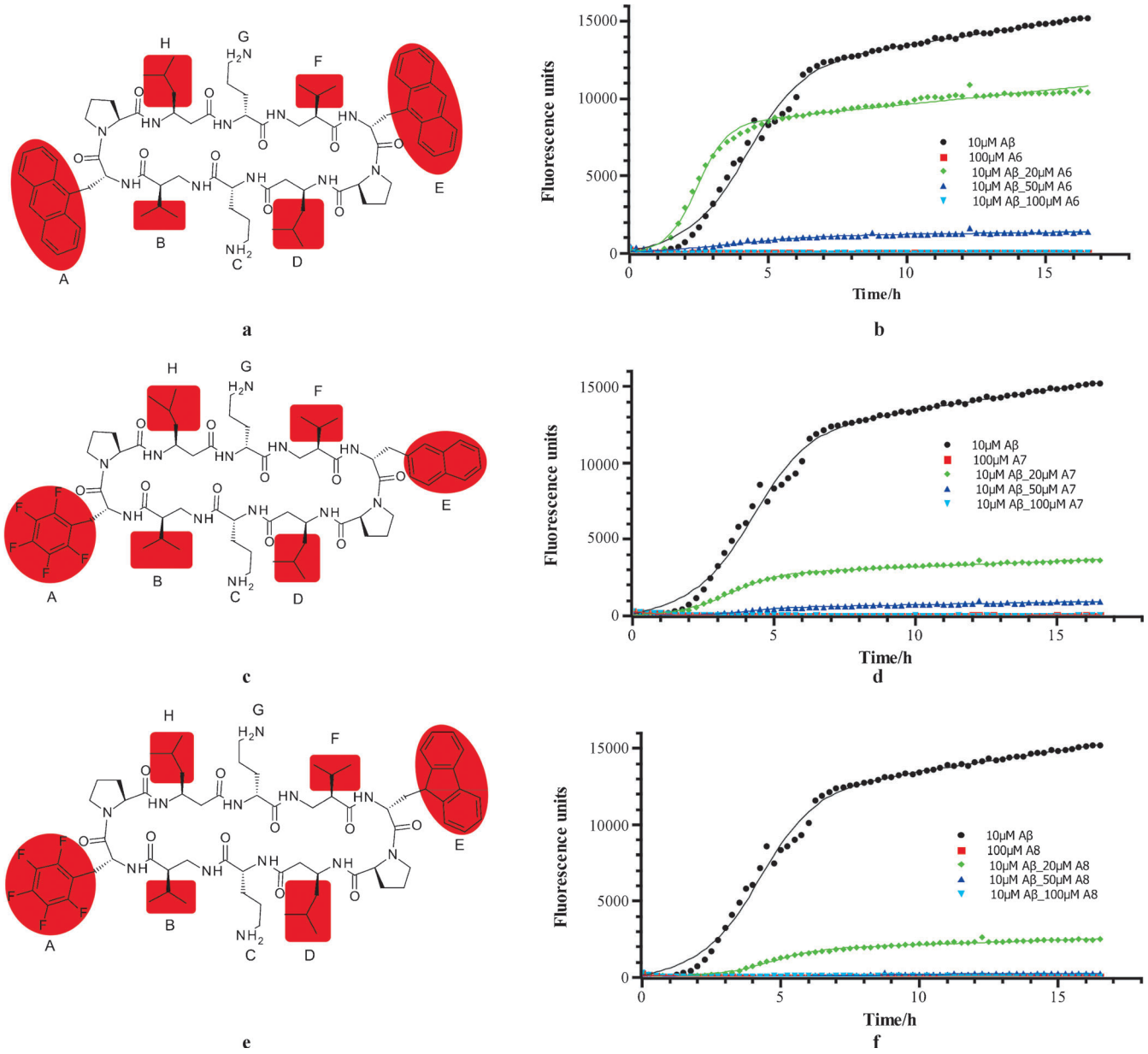

Figure 9. a), c), and e) Structures of GS analogues **6**–**8**, respectively. The modified groups based on the native GS structure are indicated in red. b), d), and f) ThT fluorescence data for Aβ(1–40) aggregation and inhibition in the presence and absence of GS analogues **6**–**8**, respectively. The concentrations of the GS analogues were 0, 20, 50, and 100 μM, and the time scale was 17 h for each measurement.

before adding 10, 30, or 60 μM GS or its analogues. After 17 h incubation of the mixtures, we measured a decrease in ThT fluorescence. On average, ThT fluorescence dropped to about 50 and 80% in the presence of 60 μM and 10 μM GS and its analogues, respectively. The samples were investigated by AFM, and we no longer observed amyloid fibrils (Figure 10b). These results strongly suggest that GS and its analogues not only prevent the aggregation of amyloid beta fibril formation but also partly dissolve the fibrils.

Conclusion

In conclusion, we found the natural macrocyclic peptide gramicidin S (**1**) to be an inhibitor of Aβ(1–40) peptide aggregation. GS-based analogues with different side chains on the β-strands and β-turns were also tested. We report these GS analogues to have different efficiencies in the inhibition of fibril formation of the Aβ peptide. The substantial differences in the fibril inhibition by native GS and analogues **2** and **3** reveal that suitable hydrophobicity on the β-strand is essential for the interactions between the Aβ peptide and the GS-based analogues. A comparison of the Aβ peptide fibril

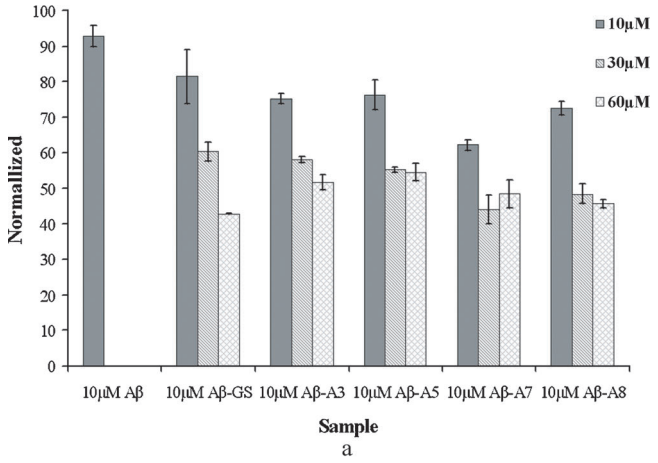

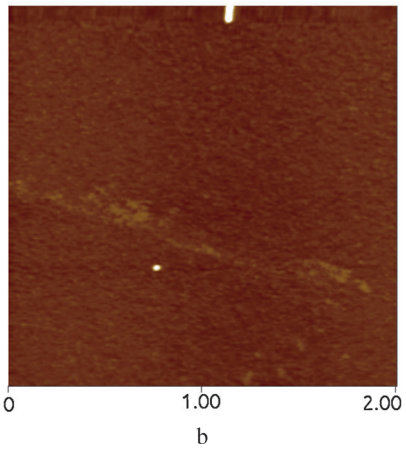

Figure 10. a) The normalized ThT fluorescence intensity of the Aβ(1–40) fibrils after incubation with different concentrations of GS and its analogues at 37 °C for 17 h. b) AFM image showing the dissolution of 50 μM amyloid fibrils by 500 μM GS (**1**) after 1 h of incubation at 37 °C.

inhibition by natural GS and analogues **4**–**8** demonstrates that the polarity and size of the facial hydrophobic side chain of the Phe residues in the β-turns is vital for inhibiting Aβ peptide fibrillization. In silico docking suggests that the binding site of GS and the GS-based analogues is located in a channel of the Aβ fibril that is surrounded by hydrophobic and hydrophilic residues. The experimentally observed trends in the ThT fluorescence assay were consistent with the predictions of our interaction models for the amyloid and inhibitor based on modeling studies. We propose that the two Phe side chains (or other aromatic groups) on the $(\alpha\beta\alpha\beta\alpha)_2$ GS-based analogues interact with the Phe side chains of the Aβ peptide by π-stacking interactions. Increasing the strength of these interactions results in more efficient inhibition of fibril formation.

Our inhibition and docking studies provide new strategies for developing inhibitors against Aβ fibril formation. Particularly encouraging in this respect is the capacity of our compounds to also dissolve preformed amyloid fibrils. The principle used in our studies could also help in the design of cyclic peptides or other compounds based on antibiotics for preventing other amyloid protein aggregation. We speculate that the channel running through the amyloid fibril may be a target for molecules that prevent the fibril from growing.

Acknowledgements

This research was financially supported by a NOW top grant (J.P.A.), the Swedish Research Council (A.G.), the Xunta de Galicia Angeles Alvariño fellowship (J.M.O.), and the European Social Fund (J.M.O.).

[1] T. Wisniewski, J. Ghiso, B. Frangione, *Neurobiol. Dis.* **1997**, *4*, 313–328.
[2] C. Ross, S. J. Tabrizi, *Lancet Neurol.* **2011**, *10*, 83–98.
[3] G. B. Irvine, O. M. El-Agnaf, G. M. Shankar, D. M. Walsh, *Mol. Med.* **2008**, *14*, 451–464.
[4] L. Haataja, T. Gurlo, C. J. Huang, P. C. Butler, *Endocr. Rev.* **2007**, *29*, 303–316.
[5] S. J. Collins, V. A. Lawson, C. L. Masters, *Lancet* **2004**, *363*, 51–61.
[6] F. Chiti, C. M. Dobson, *Annu. Rev. Biochem.* **2006**, *75*, 333–366.
[7] A. Aguzzi, T. O'Connor, *Nat. Rev. Drug Discovery* **2010**, *9*, 237–248.
[8] M. Necula, R. Kayed, S. Milton, C. G. Glabe, *J. Biol. Chem.* **2007**, *282*, 10311–10324.
[9] M. Bartolini, V. Andrisano, *ChemBioChem* **2010**, *11*, 1018–1035.
[10] M. A. Findeis, *Curr. Top. Med. Chem.* **2002**, *2*, 417–423.
[11] T. Sato, P. Kienlen-Campard, M. Ahmed, W. Liu, H. Li, J. I. Elliott, S. Aimoto, S. N. Constantinescu, J. N. Octave, S. O. Smith, *Biochemistry* **2006**, *45*, 5503–5516.
[12] C. Soto, M. S. Kindy, M. Baumann, B. Frangione, *Biochem. Biophys. Res. Commun.* **1996**, *226*, 672–680.
[13] L. O. Tjernberg, J. Naslund, F. Lindqvist, J. Johansson, A. R. Karlstrom, J. Thyberg, L. Terenius, C. Nordstedt, *J. Biol. Chem.* **1996**, *271*, 8545–8548.
[14] J. Zheng, C. Liu, M. R. Sawaya, B. Vadla, S. Khan, R. J. Woods, D. Eisenberg, W. J. Goux, J. S. Nowick, *J. Am. Chem. Soc.* **2011**, *133*, 3144–3157.
[15] C. Liu, M. R. Sawaya, P. N. Cheng, J. Zheng, J. S. Nowick, D. Eisenberg, *J. Am. Chem. Soc.* **2011**, *133*, 6736–6744.
[16] S. Sievers, J. Karanicolas, H. W. Chang, A. Zhao, L. Jiang, O. Zirafi, J. T. Stevens, J. Münch, D. Baker, D. Eisenberg, *Nature* **2011**, *475*, 96–100.
[17] R. J. Woods, J. O. Brower, E. Castellanos, M. Hashemzadeh, O. Khakshoor, W. A. Russu, J. S. Nowick, *J. Am. Chem. Soc.* **2007**, *129*, 2548–2558.
[18] M. Richman, S. Wilk, M. Chemerovski, S. K. T. S. Wärmländer, A. Wahlström, A. Gräslund, S. Rahimipour, *J. Am. Chem. Soc.* **2013**, *135*, 3474–3484.
[19] S. K. T. S. Wärmländer, A. Tiiman, A. Abelein, J. Luo, J. Jarvet, K. L. Söderberg, J. Danielsson, A. Gräslund, *ChemBioChem* **2013**, *14*, 1692–1704.
[20] P.-N. Cheng, C. Liu, M. Zhao, D. Eisenberg, J. S. Nowick, *Nat. Chem.* **2012**, *4*, 927–933.
[21] P.-N. Cheng, J. D. Pham, J. S. Nowick, *J. Am. Chem. Soc.* **2013**, *135*, 5477–5492.
[22] H. Hatcher, R. Planalp, J. Cho, F. M. Torti, S. V. Torti, *Cell. Mol. Life Sci.* **2008**, *65*, 1631–1652.
[23] M. Landau, M. R. Sawaya, K. F. Faull, A. Laganowsky, L. Jiang, S. A. Sievers, J. Liu, J. R. Barrio, D. Eisenberg, *PLoS Biol.* **2011**, *9*, e1001080.
[24] W. Q. Qiu, M. F. Folstein, *Neurobiol. Aging* **2006**, *27*, 190–198.
[25] T. Luhrs, C. Ritter, M. Adrian, D. Riek-Loher, B. Bohrmann, H. Dobeli, D. Schubert, R. Riek, *Proc. Natl. Acad. Sci. USA* **2005**, *102*, 17342–17347.
[26] L. H. Kondejewski, S. W. Farmer, D. S. Wishart, C. M. Kay, R. E. Hancock, R. S. Hodges, *J. Biol. Chem.* **1996**, *271*, 25261–25268.
[27] L. H. Kondejewski, S. W. Farmer, D. S. Wishart, R. E. Hancock, R. S. Hodges, *Int. J. Pept. Protein Res.* **1996**, *47*, 460–466.

[28] *Antibiotic and Chemotherapy*: Anti-infective Agents and Their Use in Therapy 9th ed. (Eds.: R. G. Finch, D. Greenwood, S. R. Norrby, R. J. Whitley), Churchill Livingstone, Edinburgh, **2010**, p. 356–365.
[29] V. V. Kapoerchan, A. D. Knijnenburg, M. Niamat, E. Spalburg, A. J. de Neeling, P. H. Nibbering, R. H. Mars-Groenendijk, D. Noort, J. M. Otero, A. L. Llamas-Saiz, M. J. van Raaij, G. A. van der Marel, H. S. Overkleeft, M. Overhand, *Chem. Eur. J.* **2010**, *16*, 12174–12181.
[30] V. V. Kapoerchan, A. D. Knijnenburg, P. Keizer, E. Spalburg, A. J. de Neeling, R. H. Mars-Groenendijk, D. Noort, J. M. Otero, A. L. Llamas-Saiz, M. J. van Raaij, G. A. van der Marel, H. S. Overkleeft, M. Overhand, *Bioorg. Med. Chem.* **2012**, *20*, 6059–6062.
[31] G. F. Gause, M. G. Brazhnikova, *Nature* **1944**, *154*, 703.
[32] R. L. Synge, *Biochem. J.* **1945**, *39*, 363–367.
[33] G. N. Tishchenko, V. I. Andrianov, B. K. Vainstein, M. M. Woolfson, E. Dodson, *Acta Crystallogr. Sect. D Biol. Crystallogr.* **1997**, *53*, 151–159.
[34] A. L. Llamas-Saiz, G. M. Grotenbreg, M. Overhand, M. J. van Raaij, *Acta Crystallogr. Sect. D Biol. Crystallogr.* **2007**, *63*, 401–407.
[35] M. van der Knaap, J. M. Otero, A. Llamas-Saiz, M. J. van Raaij, L. I. Lageveen, H. J. Busscher, G. M. Grotenbreg, G. A. van der Marel, H. S. Overkleeft, M. Overhand, *Tetrahedron* **2012**, *68*, 2391–2400.
[36] J. M. Otero, M. van der Knaap, A. L. Llamas-Saiz, M. J. van Raaij, M. Amorín, J. R. Granja, D. V. Filippov, G. A. van der Marel, H. S. Overkleeft, M. Overhand, *Cryst. Growth Des.* **2013**, *13*, 4355–4367.
[37] J. Luo, C.-H. Yu, H. Yu, R. Borstnar, S. C. L. Kamerlin, A. Gräslund, J. P. Abrahams, S. K. T. S. Wärmländer, *ACS Chem. Neurosci.* **2013**, *4*, 454–462.
[38] G. M. Morris, D. S. Goodsell, R. Huey, A. J. Olson, *J. Comput.-Aided Mol. Des.* **1996**, *10*, 293–304.
[39] D. S. Goodsell, G. M. Morris, A. J. Olson, *J. Mol. Recognit.* **1996**, *9*, 1–5.
[40] T. Antony, W. Hoyer, D. Cherny, G. Heim, T. M. Jovin, V. Subramaniam, *J. Biol. Chem.* **2003**, *278*, 3235–3240.
[41] J. Luo, S. K. T. S. Wärmländer, A. Gräslund, J. P. Abrahams, *Chem. Commun.* **2013**, *49*, 6507–6509.
[42] S. Afonin, U. H. N. Dürr, P. Wadhwani, J. Salgado, A. S. Ulrich, *Top Curr. Chem.* **2008**, *273*, 139–154.
[43] R. Zhang, X. Hu, H. Khant, S. J. Ludtke, W. Chiu, M. F. Schmid, C. Frieden, J. M. Lee, *Proc. Natl. Acad. Sci. USA* **2009**, *106*, 4653–4658.
[44] E. Katz, L. Demain, *Bacteriol. Rev.* **1977**, *41*, 449–474.
[45] L. M. Salonen, M. Ellermann, F. Diederich, *Angew. Chem.* **2011**, *123*, 4908–4944; *Angew. Chem. Int. Ed.* **2011**, *50*, 4808–4842.
[46] B. Y. Feng, B. H. Toyama, H. Wille, D. W. Colby, S. R. Collins, B. C. H. May, S. B. Prusiner, J. Weissman, B. K. Shoichet, *Nat. Chem. Biol.* **2008**, *4*, 197–199.

Received: April 22, 2013
Revised: September 12, 2013
Published online: November 11, 2013

